JOURNAL OF SOLID STATE CHEMISTRY **104**, 74–80 (1993)

Metal–Insulator Transitions in Anion-Excess $LaMnO_{3+\delta}$ Controlled by the Mn^{4+} Content*

M. VERELST, N. RANGAVITTAL, AND C. N. R. RAO†

Solid State and Structural Chemistry Unit and Jawaharlal Nehru Centre for Advanced Scientific Research, Indian Institute of Science, Bangalore-560 012, India

AND A. ROUSSET

Laboratoire de Chimie dex Materiaux Inorganiques, URA CNRS 1311, Universite Paul Sabatier, 31062 Toulouse Cedex, France

Received October 29, 1992; accepted November 9, 1992

$LaMnO_{3+\delta}$ samples with Mn^{4+} content up to 50% have been prepared by different methods. The structure of $LaMnO_{3+\delta}$ changes from orthorhombic to cubic (via rhombohedral) with increase in the Mn^{4+} content. $LaMnO_{3+\delta}$ samples containing greater than 20% Mn^{4+} are ferromagnetic and show resistivity maxima at a temperature T_t which is close to the ferromagnetic Curie temperature. The resistivity maximum is due to the occurrence of a metal–insulator transition. In samples heated to the same temperature, the value of T_t increases with % Mn^{4+}. For a given sample, T_t increases with the temperature of heat treatment due to the increase in particle size. The onset of ferromagnetism in $LaMnO_{3+\delta}$ accompanied by an insulator–metal transition is similar to that found in $La_{1-x}Ca_xMnO_3$ and $La_{1-x}Sr_xCoO_3$. © 1993 Academic Press, Inc.

Introduction

Modern solid state chemistry owes much to the pioneering efforts of Professor J. S. Anderson. Professor Anderson was a great solid state chemist and was one of the earliest chemists to get interested in the general problem of defects and stoichiometry in inorganic solids. His classic papers on defect thermodynamics and extended defects as well as his contributions to high resolution electron microscopy of complex solids cannot be forgotten. Important concepts such as infinitely adaptive structures were first introduced by him. He was a source of inspiration to one of the authors (C. N. R. Rao) in his formative years. This author also had the good fortune to work with Professor Anderson during his term as Commonwealth Visiting Professor at Oxford on various problems including electron microscopy of perovskite oxides. Professor and Mrs. Anderson were close friends of the Rao family. It is with great pleasure that we dedicate this article on the defect perovskite, $LaMnO_{3+\delta}$, to the memory of Professor Anderson.

---

* Dedicated to the memory of Professor J. S. Anderson, a pioneer in solid state chemistry and a dear friend of one of the authors (CNRR).

† To whom correspondence should be addressed.

0022-4596/93 $5.00

$LaMnO_3$ is an interesting anion-excess pervoskite (*1*) studied by Van Santen and Jonker (*2*) many years ago. Jonker (*3*) observed that $LaMnO_3$ was an orthorhombic compound which would become ferromagnetic if it could be obtained in the cubic structure at ordinary temperatures. A neutron diffraction study by Tofield and Scott (*4*) has thrown light on the nature of oxidative nonstoichiometry in this perovskite. The composition $LaMnO_{3.12}$ or $LaMn^{3+}_{0.76}Mn^{4+}_{0.24}O_{3.12}$ seems best described as $(La_{0.94}\square_{0.06})$ $(Mn^{3+}_{0.745}Mn^{4+}_{0.235}\square_{0.02})O_3$ with both A and B ion vacancies ($\square$) and involving the elimination of a small proportion of La_2O_3. In $(La_{1-x}M_x)_{1-y}MnO_{3+\delta}$, where M is a divalent cation such as Sr or Ca, the A-site deficiency, y, is less than 0.1 when $x = 0$ and decreases with increasing x (*5*). Depending on the Mn^{4+} content, the structure of $LaMnO_{3+\delta}$ is reported to change from orthorhombic to rhombohedral, the latter occurring at high Mn^{4+} content (*6–8*). A similar structural change is also seen in $La_{1-x}M_x(II)MnO_3$, where $M = Ca^{2+}$ or Sr^{2+}. Mn^{3+}–O–Mn^{4+} interaction is ferromagnetic and $La_{1-x}M_x(II)MnO_3$ therefore becomes ferromagnetic in the range $x = 0.1$ to $x = 0.5$; when $x > 0.5$, the material becomes antiferromagnetic just like $CaMnO_3$ (*7, 8*). $LaMnO_3$ containing a sufficiently high percentage of Mn^{4+} is also ferromagnetic and a Curie temperature of 170 K has been reported for $LaMnO_3$ with 20% Mn^{4+} (*7*).

In the ferromagnetic regime of $La_{1-x}Ca_x MnO_3$ ($x \leq 0.5$), electron hopping from Mn^{3+} to Mn^{4+} is rapid, giving rise to relatively low electrical resistivity. In the ferromagnetic phase, the resistivity increases with increase in temperature, showing a maximum at the Curie point (*8, 9*). Such variation in resistivity may be considered to represent a metal–insulator transition occurring at the ferromagnetic Curie temperature. When the Mn^{4+} content, x, is high and the material is antiferromagnetic, such resistivity behavior is not observed (*9*). We were interested in investigating the properties of parent $LaMnO_{3+\delta}$ with changing Mn^{4+} content, one of the main objectives being to explore the metal–insulator transition in the absence of doping with a divalent cation. For this purpose, we have prepared $LaMnO_{3+\delta}$ by several chemical routes, followed by treatment in air or O_2 to obtain varying Mn^{4+} content. Samples so prepared were characterized by X-ray diffraction, electrical resistance, and other measurements. Bond distances and other structural parameters have been obtained for $LaMnO_{3+\delta}$ samples with different Mn^{4+} content by Rietveld profile analysis.

Experimental

$LaMnO_{3+\delta}$ samples were prepared by the following routes: (i) a ceramic route by firing a mixture of La_2O_3 and Mn_2O_3 at 1470 K for 12 hr in air followed by sintering under the same conditions, (ii) a sol–gel route using citric acid and ethylenediamine as gelling agents for the lanthanum-manganese nitrate solution, (iii) coprecipitation as hydroxide or hydroxycarbonate, and (iv) combustion of a dried mixture of lanthanum and manganese nitrates with urea. In the last three soft-chemistry routes, decomposition (or homogenization in the case of combustion) was carried out by calcination at 1070 or 1220 K for 6 hr in air or oxygen. $LaMnO_{3+\delta}$ powders so prepared were pressed into pellets and annealed for 6 hr under the same conditions. The Mn^{4+} content was determined by redox titrations using standard ferrous and permanganate solutions.

In Table I, the Mn^{4+} content of some of the $LaMnO_{3+\delta}$ samples prepared by different methods is listed. We see that we are able to introduce Mn^{4+} upto ~40% in $LaMnO_3$. High-resolution X-ray diffraction data for these compounds were obtained in the 2θ range of 8°–80° with a STOE automatic powder diffractometer using a

TABLE I

Mn^{4+} Content in Various Samples of LaMnO$_{3+\delta}$[a]

Route	Conditions	Average % Mn^{4+}	T_t (K)
(i) Ceramic	1470 K/air	12 Sample 1	—
		10 Sample 2	—
(ii) Sol–gel	1070 K/air	40	215
	1070 K/O$_2$	39	222
	1220 K/O$_2$	26 Sample 1	232
		28 Sample 2	245
(iii) Hydroxide	1070 K/air	32	155
	1070 K/O$_2$	35 Sample 1	165
		33 Sample 2	145
	1070 K/N$_2$	unstable	—
	1220 K/air	26	205
	1220 K/N$_2$	5 (after 1 week)	—
Hydroxycarbonate	1070 K/air	14	—
	1220 K/air	30	255
	1220 K/O$_2$	33	287
(iv) Combustion	1070 K/air	34	165
	1220 K/air	29	205

[a] The % Mn^{4+} values have an experimental uncertainty of ±2.

Ge(111) monochromator and Cu$K\alpha$ (λ = 1.5406 Å) radiation, with a linear PSD in the transmission mode. Rietveld profile analysis was carried out on samples with Mn^{4+} content of 10%, 28%, and 40%. Electrical measurements were carried out on sintered pellets by the four-probe method in the 15–300 K range. The room-temperature resistivity of LaMnO$_{3+\delta}$ samples with ~20% Mn^{4+} was around 5 Ω cm or less; with 10% Mn^{4+}, the resistivity was much higher (~80 Ω cm). Magnetization measurements were carried out on representative samples to determine the Curie temperatures.

Results and Discussion

In Fig. 1 we have shown the X-ray diffraction patterns of three LaMnO$_{3+\delta}$ samples with different percentages of Mn^{4+}. LaMnO$_{3+\delta}$ is orthorhombic (*Pbnm*) up to ~20% Mn^{4+} and becomes rhombohedral ($R\bar{3}c$) at higher Mn^{4+} content. When the Mn^{4+} content is greater than 30%, the rhombohedral angle becomes close to 90° and the diffraction pattern is that of a cubic phase (*Fm*3*m*). In Table II we list the unit cell parameters of typical LaMnO$_{3+\delta}$ samples studied by us. The unit cell dimensions, as well as the properties of LaMnO$_3$, seem to depend not only on the Mn^{4+} content but also on the heat treatment as shown later.

The structure of LaMnO$_{3+\delta}$ samples with 10%, 28%, and 40% Mn^{4+} and possessing the orthorhombic (*Pbnm*, z = 4), rhombohedral ($R\bar{3}c$, z = 2), and cubic (*Fm*3*m*, z = 8) structure, respectively, was subjected to Rietveld profile analysis. The lattice parameters of these perovskites are Mn^{4+} ~ 10%, a = 5.543(2), 5.495(2), and 7.804(5) Å; Mn^{4+} ~ 28%, a = 5.479(1) Å, α = 60.54(1)°; and Mn^{4+} ~ 40%, a = 7.792(14) Å. The Mn–O distances in these compounds show interesting variation with % Mn^{4+}. In the orthorhombic sample with 10% Mn^{4+}, there are two Mn–O distances of 2.023 and 2.058

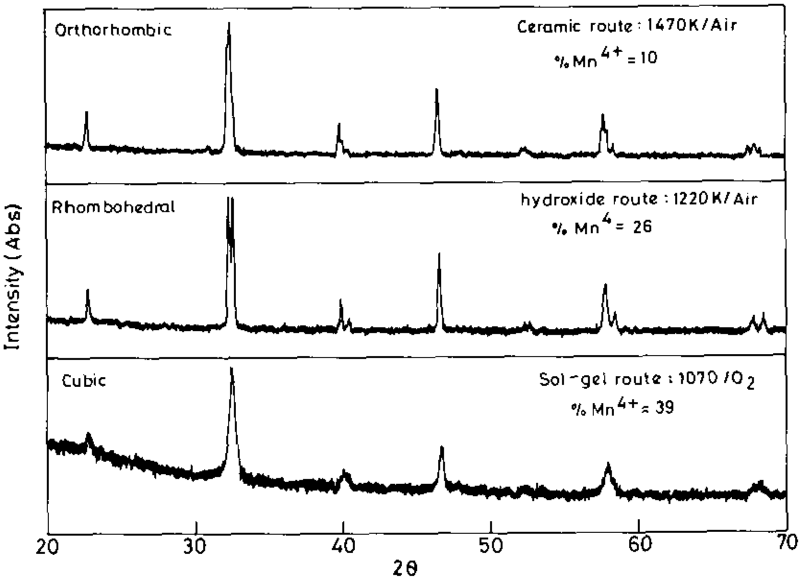

FIG. 1. X-ray diffraction patterns of $LaMnO_{3+\delta}$ with different percentages of Mn^{4+}.

Å; these are close to the sum of the ionic radii of Mn^{3+} and O^{2-} (2.01 Å). The Mn–O distance in the rhombohedral sample with 28% Mn^{4+} is 1.957 Å, while that in the cubic sample is 1.948 Å. The distance of 1.948 Å is close to the sum of ionic radii of Mn^{4+} and O^{2-} (1.92 Å). The La–O distance also varies with % Mn^{4+} with distances in the range 2.98 and 2.25 Å in the orthorhombic structure, and in the 2.98–2.54 Å range in the rhombohedral structure. In the cubic structure, it is 2.756 Å. The octahedral dis-

TABLE II

STRUCTURE AND PROPERTIES OF $LaMnO_{3+\delta}$ SAMPLES PREPARED BY DIFFERENT METHODS

Preparative route	Mn^{4+}	Structure[a]	Unit cell parameters	T_t (K)[b]
Ceramic 1470 K/air	10	O (*Pbnm*)	a = 5.515; b = 5.502; c = 7.880 Å	—
Hydroxide 1220 K/air	26	R ($R\bar{3}c$)	a = 5.480; α = 60.566°	205
Sol–gel 1220 K/O_2	28	R ($R\bar{3}c$)	a = 5.476 Å, α = 60.564	245
Hydroxycarbonate 1220 K/O_2	33	C (*Fm*3*m*)	a = 7.788 Å	280
Hydroxide 1070 K/air	32	C (*Fm*3*m*)	a = 7.787 Å	155
Sol–gel 1070 K/O_2	39[c]	C (*Fm*3*m*)	a = 7.792 Å	222

[a] O, Orthorhombic; R, Rhombohedral; C, Cubic.

[b] The ferromagnetic T_c values obtained from magnetization measurements are generally 10–15° higher.

[c] A sample prepared by the sol–gel route with ~50% Mn^{4+} showed the same structure.

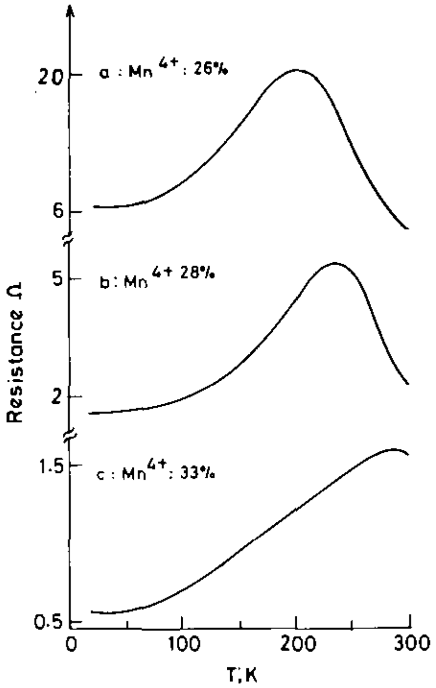

FIG. 2. Variation of electrical resistance with temperature in $LaMnO_{3+\delta}$ samples annealed at 1220 K. Note that the temperature corresponding to the resistance maximum increases with the Mn^{4+} content.

tortion decreases from the orthorhombic structure to the cubic structure as evidenced by the Mn–O–Mn angle. The Mn–O–Mn angle in the orthorhombic and rhombohedral structures is 149.56° and 167.10°, respectively, while it is 180° in the cubic structure.

We have studied the electrical properties of $LaMnO_{3+\delta}$ samples annealed at 1070 and 1220 K. All the samples containing more than 20% Mn^{4+} and possessing the rhombohedral or cubic structure show the metal–insulator transition around the Curie temperature. In Fig. 2 we show the electrical resistance behavior of typical samples heated to 1220 K with % Mn^{4+} greater than 20. All the samples exhibit characteristic resistance maxima. The temperature corresponding to the resistance maximum, T_t, is close to the Curie temperature. What is interesting is that T_t increases as the Mn^{4+} content increases. This is exactly what we would expect since the ferromagnetic Curie temperature also increases in the same manner. In $La_{1-x}M_x(II)MnO_{3+\delta}$ the material becomes antiferromagnetic when $x > 0.5$. In $LaMnO_{3+\delta}$, however, we are not able to increase the Mn^{4+} content beyond ~50% and the material remains ferromagnetic in the % Mn^{4+} range of 20 to 50.

In Tables I and II we have listed the values of the metal–insulator transition temperatures for the different $LaMnO_{3+\delta}$ samples prepared by us. In Fig. 3 we have plotted the transition temperature, T_t, against the Mn^{4+} content for samples heated to 1070 and 1220 K. We see that within the experimental uncertainties, the value of T_t is proportional to the Mn^{4+} content. Furthermore, T_t is also dependent on the temperature of heat treatment. The slopes of the plots corresponding to the two temperatures of treatment (Fig. 3) are, however, comparable. Part of the reason for the variation of T_t or the Curie temperature with the temperature of heat treatment could be the complex defect structure involving anion excess as well as *A*- and *B*-ion vacancies (*3*, *4*). It is more likely, however, that the T_t is

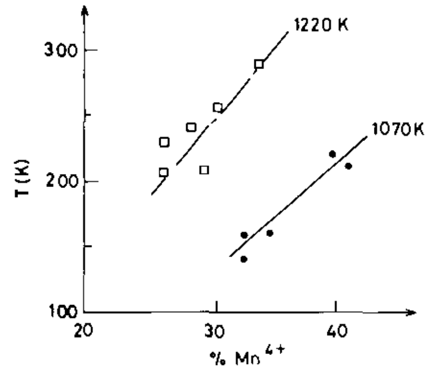

FIG. 3. Variation of the temperature of the metal–insulator transition, T_t, of $LaMnO_{3+\delta}$ with Mn^{4+} content. Data at two annealing temperatures are plotted.

TABLE III

EFFECT OF ANNEALING TEMPERATURE ON THE PROPERTIES OF $LaMnO_{3+\delta}$ PREPARED BY THE SOL–GEL ROUTE

Heat treatment temperature (K)	% Mn^{4+}	Surface area (m^2/g)	T_t (K)
870	52(C)	25	50[a]
970	42(C)	20	190
1070	37(C)	10	215
1220	26(R)	3	233
1370	18(O)	<1	—[b]
1470	10(O)	<1	—

[a] Broad transition.

[b] No clear transition.

lower for samples heated at a lower temperature (for the same Mn^{4+} content) because of particle size effects.

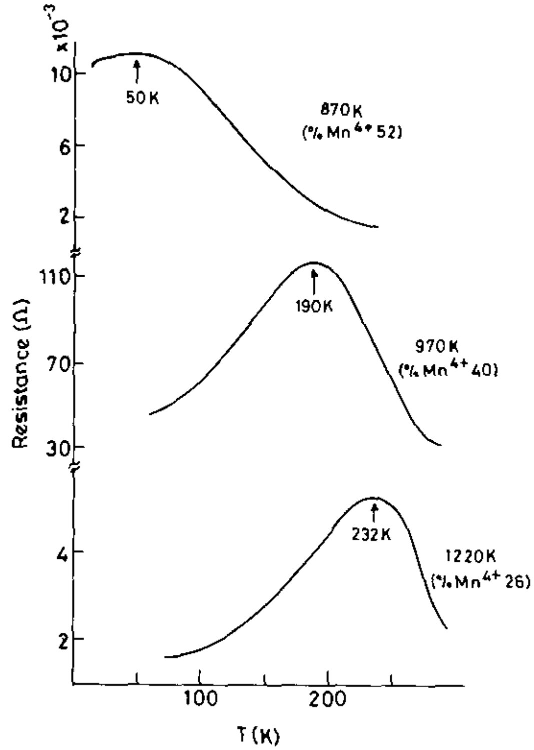

FIG. 5. Temperature variation of electrical resistance of $LaMnO_{3+\delta}$ samples annealed at different temperatures. Note the increase in T_t with increased annealing temperature.

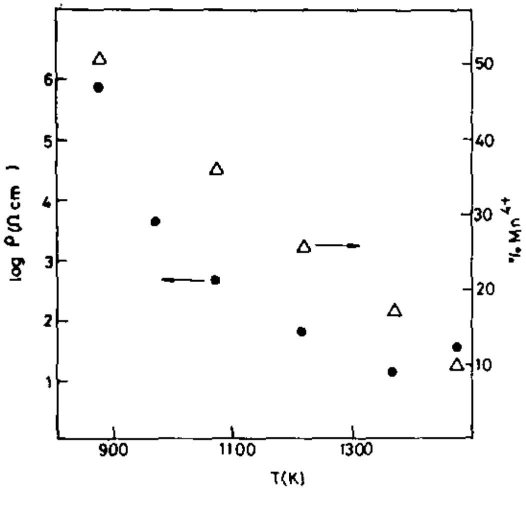

FIG. 4. Variation of (a) the Mn^{4+} content (triangles) and (b) the 300 K resistivity (closed circles) of $LaMnO_{3+\delta}$ prepared by the sol–gel route.

In order to investigate the effect of particle size on the metal–insulator transition, we have examined $LaMnO_{3+\delta}$ samples prepared by the sol–gel route and heated to different temperatures. The Mn^{4+} content of the sample decreases with increase in the temperature of heat treatment (Table III, Fig. 4). The surface area decreases with increase in temperature of heat treatment due to the increase in particle size as expected. Electrical resistivity also decreases appreciably with the increase in the treatment temperature (see resistivity data shown in Fig. 4). What is interesting is that the temperature of the metal–insulator transition, T_t, increases markedly with the increase in the temperature of treatment although the Mn^{4+} content decreases from 52% to 26% (Fig. 5). This is clearly a particle size effect. It is indeed known that magnetization decreases markedly when the particle size is small. Accordingly, the sample heated to 870 K shows a broad transition at a low temperature (~50 K) although it contains around

50% Mn^{4+}. Similarly, the sample heated to 970 K with ~40% Mn^{4+} shows a T_t of 190 K (compared to 222 K for a sample heated to 1070 K with 39% Mn^{4+}).

Ferromagnetism and the metal–insulator transition occur around the same temperature in $LaMnO_{3+\delta}$ and $LaM_x(II)Mn_{1-x}O_3$ because the electrons responsible for ferromagnetism are also involved in the conduction process (*8, 9*). These oxides are itinerant-electron ferromagnets, where electron-hopping from Mn^{3+} to Mn^{4+} is responsible for the relatively low resistivity as well as the ferromagnetism. The situation is comparable to that in $La_{1-x}Sr_xCoO_3$ (*10*), where electron hopping between Co^{3+} and Co^{4+} causes metallicity as well as ferromagnetism. Interestingly, in the cobalt system, at $x \approx 0.15$, ferromagnetism sets in at low temperatures and the *d*-electrons become itinerant at this composition even at room temperature. The explanation for the resistivity maximum in $LaMnO_{3+\delta}$ is as follows. $LaMnO_{3+\delta}$ containing a sufficiently high proportion of Mn^{4+} has low resistivity at ordinary temperatures, but as the temperature is decreased, the resistivity increases just as in many oxide semiconductors. However, at the Curie temperature, the faster electron hopping between Mn^{3+} and Mn^{4+} reduces the resistivity, giving metal-like behavior in the ferromagnetic regime at low temperatures.

Acknowledgment

The authors thank the Indo-French Centre for the Promotion of Advanced Research for support.

References

1. C. N. R. Rao and J. Gopalakrishnan, "New *Directions in Solid State Chemistry*," Cambridge Univ Press, London/New York (1989).
2. J. H. Van Santen and G. H. Jonker, *Physica* **16,** 599 (1950).
3. G. H. Jonker, *Physica* **22,** 707 (1956).
4. B. C. Tofield and W. R. Scott, *J. Solid State Chem.* **10,** 183 (1974).
5. Y. Takeda, T. Kojima, R. Kanno, N. Imanishi, G. O. Shen, O. Yamatoto, M. Mori, C. Asakawa, and T. Abe, *Mater. Res. Bull.* **26,** 156 (1991).
6. A. Wold and R. J. Arnott, *J. Phys. Chem. Solids* **9,** 176 (1959).
7. E. O. Wollan and W. C. Koehler, *Phys. Rev.* **100,** 549 (1955).
8. J. B. Goodenough, *Prog. Solid State Chem.* **5,** 149 (1971).
9. J. Tanaka, M. Omehara, S. Tamura, M. Tsukioka, and S. Ehara, *J. Phys. Soc. Jpn.* **51,** 1236 (1982).
10. C. N. R. Rao, D. Bahadur, O. Parkash, and P. Ganguly, *J. Solid State Chem.* **22,** 353 (1977).